OPEN ACCESS
Journal of Multidisciplinary Applied Natural Science Vol. 6 No. 1 (2026) https://doi.org/10.47352/jmans.2774-3047.318
Check for updates
Research Article

Optimization of Graphene Oxide-Based Dispersive Solid-Phase Extraction from Cassava Peel Using Response Surface Methodology for Determining Ciprofloxacin Antibiotic Residues

Rinawati Rinawati*, Elsa Fitrianingsih, Dian Rifani Muthia, Siti Salwa Khotijah, Agung Abadi Kiswandono, Widiarti Widiarti, Achmad Gus Fahmi, and Tarmizi Taher

Received : July 15, 2025	Revised : September 29, 2025	Accepted : October 13, 2025	Online : November 2, 2025

Abstract
Pharmaceutical waste containing antibiotics is a major contributor to water pollution. The widespread use of ciprofloxacin (CIP), an antibiotic, causes residues to accumulate in the environment, especially in aquatic habitats, causing ecological damage. A dispersive solid-phase extraction (DSPE) method was selected to trace CIP residues in the natural environment. Graphene oxide (GO) serves as an absorbent in the DSPE procedure. To achieve the best results, an evaluation is needed to identify the most favorable absorption conditions for CIP. This study used a modified Hummers method to produce GO from cassava peel waste, which contains a lot of carbon and cellulose. Then the GO was characterized by Fourier transform infrared (FTIR) spectroscopy, X-ray diffraction (XRD), Raman spectroscopy, and scanning electron microscopy (SEM). The response surface method (RSM) was based on a Box-Behnken Design (BBD). The CIP adsorption conditions were determined by considering the adsorbent dosage, pH, CIP concentration, and contact time. The adsorption capacity of 99.87% was achieved under the following conditions: pH 4.4; contact time of 35.2112 min; concentration of CIP 619.119 ppb; and adsorbent dosage 23.3237 mg. The method demonstrated linearities R^2 of 0,9987 with a detection limit of 4.05 ppb and a quantification limit of 13.50 ppb, and %RSD in the range 3–5%, and recovery of 98.90%. It confirms that GO from cassava peel waste has the potential to be an adsorbent for the antibiotic CIP. This study provides a novel approach by employing cassava peel-derived GO for DSPE, achieving nearly complete CIP removal (99.87%), thereby offering a sustainable and highly sensitive method for environmental monitoring.

Keywords: cassava peel, ciprofloxacin antibiotic, dispersive solid-phase extraction, graphene oxide, response surface methodology

1. INTRODUCTION

The issue of water contamination has become a prominent global concern. Pharmaceutical waste significantly contributes to water pollution. People commonly use ciprofloxacin (CIP), a second-generation fluoroquinolone antibiotic, to treat Gram -negative bacterial infections like Escherichia coli and Salmonella spp., as well as Gram-positive infections like Staphylococcus aureus [1][2]. The widespread utilization and production of CIP can lead to the buildup of residues in the environment, especially in the aquatic ecosystems. The aquatic environment has discovered CIPs due to their remarkable stability and solubility in water, even at different pH levels. The global mean concentration of CIP in surface water varies from 10 to 100,000 ng/L, with lakes having the highest levels, ranging from 2.5 to 6.5 mg/L [3]. Accumulation of CIP residues can have detrimental effects, including reducing bacteria's capacity to create dangerous compounds, causing environmental harm, hindering animal cartilage development, and spreading diseases such as skin and intestinal infections. Therefore, it is crucial to carefully observe and track the presence of CIP residues, especially in aquatic environments, to prevent adverse impacts on human health and ecosystem endowment levels [4][5].

Currently, scientists have developed techniques sampel preparation, examples include solid-phase extraction (SPE) and disperse SPE (DSPE), to effectively and securely monitor antibiotics in the environment [6][7]. Nevertheless, the use of SPE technologies is associated with column obstruction, complexity, high costs, time-consuming procedures, and a lack of repeatability [8]. The DSPE approach was chosen because it has several advantages over traditional SPE procedures, including lower solvent

Table 1. Selected levels of independent variables in BBD design.

Influencing Factors	-1	0	+1
Adsorbent dose (mg)	10	20	30
pH (-)	2	6	10
Contact time (min)	10	35	60
CIP concentration (ppb)	300	650	1000

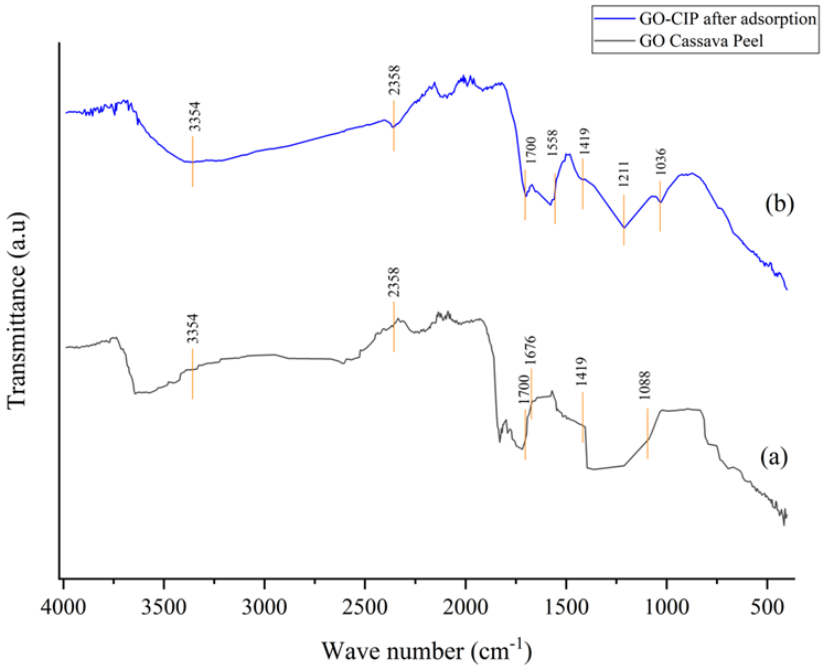

Figure 1. The FTIR spectra of (a) GO and (b) GO-CIP after adsorption.

usage, lower cost, and faster sample preparation time. The DSPE approach uses sorbents to isolate the analytic from its matrix. Mesoporous materials or nanomaterials, such as graphene oxide (GO) can be employed as adsorbents to eliminate antibiotic waste [6][9]. Several studies have demonstrated that GO can be utilized to adsorp antibiotics such as ceftriaxone, CIP, norfloxacin, and lemofloxacin [10]-[12].

GO is conventionally synthesized using non-renewable mineral resources, rendering its production process unsustainable. In pursuit of more cost-effective and sustainable alternatives, researchers have explored potential materials, such as agricultural waste, which is abundant, cheap, and renewable. In Lampung, cassava production yields an average of 25 tons/ha during harvest, generating significant cassava peel waste [13]. The part that is used is the outer layer of the cassava skin, which is brown-red in color and is usually considered waste [14]. Cassava skin has a fairly high carbon content of 59.31% and cellulose of 43.426%. With this high carbon content, cassava skin can be utilized to become GO [15]. This study employed the modified Hummers method to produce GO. Fourier transform infrared (FTIR), scanning electron microscopy (SEM) and X-ray diffraction (XRD) were carried out for its characterization. As a result, cassava peel GO has the potential to be a promising adsorbent for treating CIP antibiotic residues [14] [15].

Several parameters, including pH, GO adsorbent dose, contact time, and CIP concentration, can help achieve optimal conditions for CIP adsorption in the aquatic environment. The RSM approach can optimize CIP adsorption conditions. The RSM technique surpasses standard optimization methods in terms of efficiency, effectiveness, and cost-effectiveness [16]. Multiple studies have demonstrated that using RSM can improve the process of adsorption of heavy metals, methadone, methylene blue, and textile waste in water bodies.

The RSM technique is employed to determine the optimal state, the interaction of several parameters, and their influence on CIP adsorption [17]-[19]. Therefore, this study introduces cassava peel waste as a novel, low-cost, and sustainable precursor for the synthesis of GO, which is subsequently applied in the solid phase of the DSPE method for CIP analysis. Unlike previous studies, this work highlights the unique use of cassava peel as an eco-friendly carbon source, integrates response surface methodology (RSM) to optimize multiple parameters simultaneously. The main contribution of this research lies advancing the development of eco-friendly adsorbent materials while demonstrating their practical applicability in analytical methods for environmental monitoring.

2. MATERIALS AND METHODS

2.1. Materials

The present study used analytical-grade chemicals without any further purification. Hexpharm Jaya supplied the CIP antibiotic to prepare the standard solution. Additional chemicals, including concentrated sulfuric acid (H_2SO_4), iron (III) chloride hexahydrate ($FeCl_3 \cdot 6H_2O$), methanol (CH_3OH), 30% hydrogen peroxide (H_2O_2), triethanolamine ($C_6H_{15}NO_3$), and acetonitrile (C_2H_3N), were acquired from Supelco Sigma Aldrich and utilized without further modification. The chemicals utilized in this research included barium chloride ($BaCl_2$, Merck TM), potassium permanganate ($KMnO_4$, Merck TM), 37% hydrochloric acid (HCl, Smart-Lab), sodium hydroxide (NaOH, Merck TM), and distilled water. Local farmers in Lampung Province provided the raw material for the study, which was cassava peel waste.

The experiment relied on several instruments, such as an analytical balance (AND HR-150A, with a capacity of 152 g and a precision of 0.1 mg), a pH meter (Water Tester EZ-9901), a hot plate magnetic stirrer (Stuart Biocote R200000 685), an ultrasonic device (1510 Branson), a centrifuge (Fischer Scientific 1827001027164), and an oven (Memmert 55). The resulting GO material was characterized using advanced analytical instruments, including the XRD apparatus (XPERT PRO Panalytical PW3040/60), the FTIR instrument (Agilent Cary 630), and the SEM apability (EVO® MA 10). The determination of CIP concentration in various samples was carried out using Shimadzu LC-2050C high performance chromatography (HPLC) equipment.

2.2. Methods

2.2.1. Preparation of Bio Graphite from Cassava Peel Waste

The cassava peel waste was thoroughly washed with water to remove any contaminants. The pristine cassava peel waste was thereafter sliced into small fragments and left to desiccate for a period of 24–36 h in the sun. After the initial drying step, the cassava peels were subjected to a second drying process in an oven at 100 °C for a duration of 1.5 h. Once the cassava peels had completely dried, they were fragmented into smaller fragments and placed into a crucible cup, with a total weight of around 6 g. The crushed material underwent a

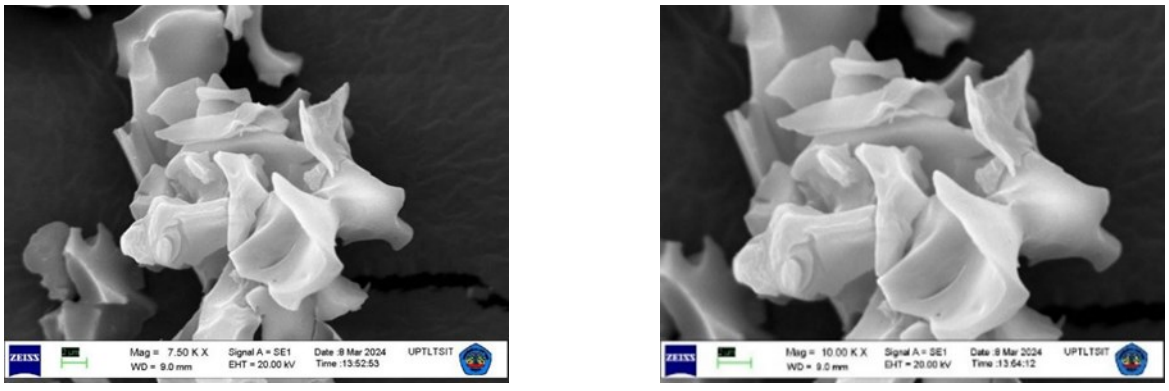

(a) **(b)**

Figure 2. SEM images of GO at magnifications of (a) 7500× and (b) 10,000×.

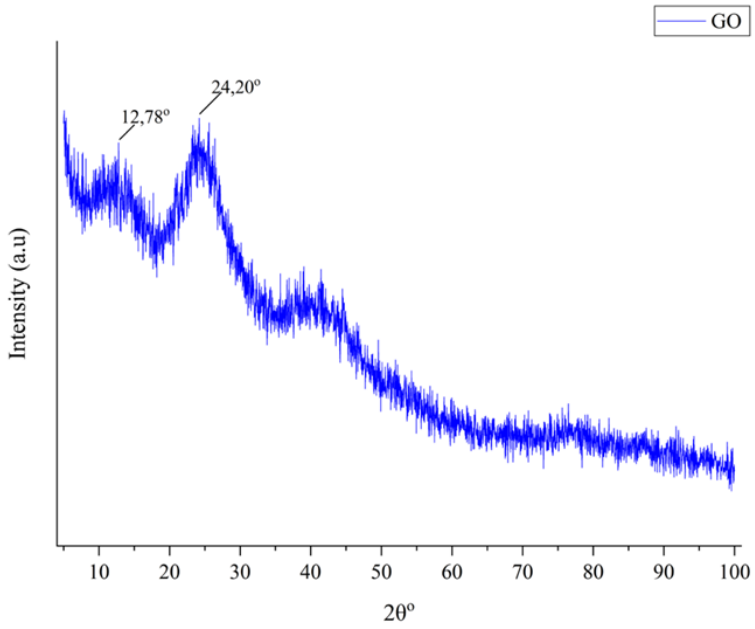

Figure 3. The XRD spectrum of GO cassava peel waste.

high-temperature treatment, reaching a maximum temperature of 350 °C, which was maintained for a duration of 2 h. After cooling in a desiccator for 15 min, the material was crushed with a mortar and pestle before passing through a 100-mesh sieve. A 5 g of the final carbon material from the previous step were weighed and added to 1 L. Then, 500 mL of distilled water was added to the beaker, and a magnetic stirrer was used to agitate the mixture at 600 rpm. A 4 mL of $FeCl_3 \cdot 6H_2O$ solution was added to this suspension [20]. The mixture was retained at room temperature and the stirring speed was increased to 900 rpm. A 1 M HCl was gradually added to the combined solution until the pH was nearly adjusted to two. At 60 °C, the stirring was maintained for 5 h. The graphite precipitate was then separated from the supernatant using centrifugation. After washing the precipitate with distilled water until it achieved a neutral pH of 7, it was filtered through filter paper. After that, the precipitate was dried in an oven for 8 h at 50 °C and 5 h at 110 °C. Furthermore, a desiccator was used to cool the dry material for 15 min [21].

2.2.2. Preparation of GO using the Modified Hummers Method

Graphite, weighing 1 g, was mixed with 23 mL of concentrated H_2SO_4 in a 500 mL beaker to create GO. The liquid was continually agitated using a magnetic stirrer and maintained at a low temperature in an ice bath for a duration of 30 min. Subsequently, a total of 3 g of $KMnO_4$ were gradually added into the mixture, ensuring that the temperature stayed below 10 °C. The agitation was thereafter sustained for an additional 30 min at 35 °C. The temperature of the combination was raised gradually by adding 46 mL of distilled water until it reached 98 °C. After reaching the intended temperature, the mixture was left at room temperature for approximately 15 min [22][23]. In order to enhance the effectiveness of the oxidation reaction, a volume of 140 mL of distilled water was introduced into the mixture. During a 10-min period of stirring using a magnetic stirrer, 10 mL of a 30% H_2O_2 solution was added gradually. The resulting suspension was thoroughly washed multiple times with a 5% HCl solution in order to eliminate the sulfate ions. Testing with a $BaCl_2$ solution confirmed the suspension's absence of sulfate ions, as evidenced by the absence of a white precipitate. The object was thoroughly cleaned with distilled water until it reached a pH of 5. The solution was thereafter subjected to centrifugation at a speed of 5000 rpm for 10 min in order to isolate the precipitates. The resulting solid was dispersed in 450 mL of distilled water, subjected to sonication for 30 min, and subsequently filtered using filter paper. The isolated precipitate was subsequently dehydrated at 60 °C for 5 h [22][23].

2.2.3. Characterization of GO

The GO material underwent a thorough analysis using a diverse range of analytical instruments to figure out its properties and characteristics. An FTIR instrument identified the functional group of GO. The SEM was used to analyze the morphological properties, elemental content, and quantitative composition of the GO. An XRD technique was employed to examine the structural organization and crystalline properties of the GO material and assess its level of crystallinity.

2.2.4. Standard Preparation

A solution was prepared by dissolving 25 mg of CIP·HCl in 50 mL of mobile phase. The solution was diluted at a ratio of 1:2 to achieve concentrations of 60, 80, 100, and 250 ppb of the reference solution.

2.2.5. Chromatographic Condition

An isocratic elution was performed using a mobile phase composed of 1% triethanolamine buffer and 80% acetonitrile (97:3 ratio). Before use,

Table 2. The results of the BBD.

Run	Adsorbent Dose (mg)	CIP concentration (ppb)	pH	Contact time (min)	%Adsorption
1	20	650	2	10	90.02
2	20	1000	2	35	97.37
3	20	650	6	35	95.91
4	30	650	6	10	95.84
5	10	1000	6	35	96.65
6	20	300	2	35	91.38
7	30	650	10	35	19.77
8	10	650	6	60	95.89
9	20	650	6	35	95.76
10	20	1000	10	35	33.01
11	10	650	6	10	95.47
12	30	650	6	60	95.48
13	20	1000	6	10	96.58
14	30	1000	6	35	97.04
15	10	650	2	35	95.51
16	10	300	6	35	90.43
17	20	1000	6	60	97.08
18	20	650	6	35	95.60
19	20	650	6	35	95.59
20	20	650	6	35	95.75
21	20	300	10	35	91.67
22	20	300	6	10	90.54
23	20	300	6	60	95.74
24	30	300	6	35	90.63
25	20	650	10	10	79.87
26	20	650	2	60	95.49
27	30	650	2	35	94.11
28	10	650	10	35	19.08
29	20	650	10	60	41.88

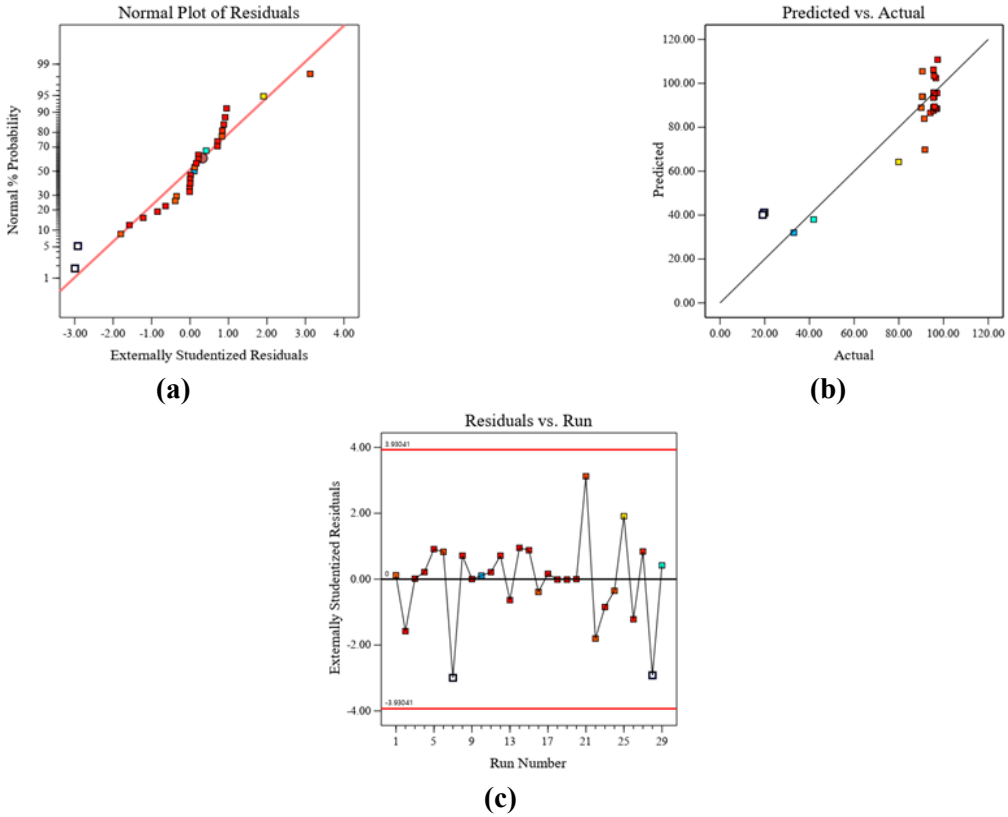

Figure 4. (a) Normal probability of student residuals, (b) residuals versus predicted, and (c) residuals versus run number.

we filtered it using a 0.45-µm nylon disc filter (Millipore) and sonicated it for 20 min. The rate of flow was 1.2 mL/min, and the volume injected was 20 µL. The separation was achieved using a Hypersil C18 column with dimensions of 4.6 × 150 nm and a particle size of 5 µm. The separation was carried out at 25 °C using a PDA detector [24].

2.2.6. Experimental design of Box Behnken Design (BBD)

BBD was used for the experiment. This method involves changing variables at three levels: high (+1), middle (0), and low (-1), along with five extra central replication points, which can be seen in Table 1. The BBD design generated 29 tests using the supplied parameters. These experiments were meticulously and precisely organized using Design-Expert software (DX13).

The study involved conducting tests in a sequential manner, following the values pointed out in Table 1 of the BBD design. Each sample consisted of a combination of a certain concentration of the antibiotic CIP solution with a defined quantity of the GO adsorbent. This combination took place under controlled pH conditions and for a specified duration of contact. The GO was subsequently isolated through the process of centrifugation and filtration, enabling the determination of the residual antibiotic concentration in the solution using HPLC. A fitness analysis was conducted to ascertain the accuracy and reliability of the obtained data. Equation (1) designated the response variable as the percentage of antibiotic adsorption;

$$Adsorption\,(\%) = \frac{Co - Cx}{Co} \times 100\% \quad \textbf{(1)}$$

Where C_0 and C_x represent the initial and final concentrations of CIP in solution (ppb). The analytical method was validated by determining the calibration curve, linearity, %recovery, repeatability, relative standard deviation percentage (%RSD), detection limit (LOD), and quantification limit (LOQ). The calibration curve was constructed using standard CIP solutions at concentrations of 60, 80, 100, and 250 ppb. Linearity was evaluated by plotting concentration versus peak area, yielding a correlation coefficient (R^2) greater than 0.999.

The LOD and LOQ values were calculated according to International Council for Harmonisation of Technical (ICH) guidelines using the formulas LOD = 3.3 × (σ/S) and LOQ = 10 × (σ/S), where σ is the standard deviation of the response and S is the slope of the calibration curve.

3. RESULTS AND DISCUSSIONS

3.1. GO Characterization

The GO produced was analyzed using XRD, SEM, and FTIR techniques. Fig. 1 displays the results of adsorption characterization using FTIR for GO and GO-CIP. Following CIP adsorption, certain GO peaks remain constant. These findings suggest that adsorption does not alter substance structure. The results of the GO and GO characterization after adsorption (Fig. 1(a) and 1(b)) reveal the presence of C–O–C stretching vibrations at wavelengths 1036 and 1088 cm-1, respectively. Additionally, vibrations at 1419 cm-1 indicate C–H bending, while vibrations at 1676 and 1700 cm-1 indicate aromatic C=C and C=O stretching vibrations at COOH, respectively [25][26]. The presence of an additional signal at 1211 cm-1 indicates CIP has been well adsorbed into GO, as demonstrated by the adsorption of the C–F group on CIP [27][28]. The signal at 1558 cm-1 corresponds to the N–H bending motion of the secondary amine [29]. The FTIR spectra demonstrate the effective method of producing GOs, as they exhibit functional groups that are appropriate for pure GO. Sujiono and Surekha discovered that GO consists of oxygen-based functional groups such as epoxy (C–O–C), carbonyl (C=O), carboxyl (COOH), and hydroxyl (O–H). The observation of the C–F group of CIP and the N–H bending group of secondary amine at 1211 cm-1 indicates the successful attachment of CIP to GO. Unfortunately, the characterization results did not reveal the presence of any C–N group, necessitating more analysis [30][31].

Fig. 2 presents the SEM morphology of GO,

Table 3. Results of analysis of variance (ANOVA).

Source	Sum of Squares	dF	Mean Square	F-Value	P-Value
Model	12870.91	14	919.35	4.80	0.0029*
A-Adsorbent dose of GO	0.0018	1	0.0018	9.458E-06	0.9976
B-CIP concentration	88.87	1	88.87	0.4637	0.5070
C-pH	6467.58	1	6467.58	33.75	<0.0001*
D-Contact time	59.70	1	59.70	0.3115	0.5856
AB	0.0091	1	0.0091	0.0000	0.9946
AC	1.09	1	1.09	0.0057	0.9409
AD	0.1537	1	0.1537	0.0008	0.9778
BC	1044.97	1	1044.97	5.45	0.0349*
BD	5.51	1	5.51	0.0287	0.8678
CD	472.50	1	472.50	2.47	0.1387
A^2	354.67	1	354.67	1.85	0.1952
B^2	53.87	1	53.87	0.2811	0.6043
C^2	3889.60	1	3889.60	20.30	<0.0005*
D^2	62.46	1	62.46	0.3259	0.5771
Residual	2683.11	14	191.65		
Lack of Fit	2683.11	10	268.30	15961.28	<0,0001*
Pure Error	0.0672	4	0.0168		
Cor Total	15554.02	28			

*Significant

Table 4. Fit statistic.

Std. Dev.	Average	C.V (%)	R^2	Adjusted R^2	Predicted R^2	Adeq Precision
13.84	85.00	16.29	0.8275	0.6550	0.0064	7.9102

where at 7,500× magnification the sheets appear fragmented with thin, peeling layers, while at 10,000× magnification the surface resembles a stack of thin leaves with relatively flat regions and slightly wavy creases. This morphology indicates that exfoliation occurred during the oxidation and ultrasonication processes, producing thin layered structures typical of GO. The presence of folds, wrinkles, and stacked sheets confirms the wide surface area and peeling sheet characteristics reported by Rinawati et al. [10] , although partial agglomeration still occurs due to interlayer interactions.

The GO cassava peel was characterized using XRD. The results showed an amorphous difractogram (Fig. 3) with two main peaks at 12.78° and 24.20°, indicating a carbon-based substance. The 2θ peak at 12.78° is a characteristic of the material GO. This is in line with the study by Donato et al. [32], where GO has characteristics with a peak 2θ ranging from 9° to 12°. According to Rinawati et al. [10], the GO difractogram pattern manufactured from corncob creates a 2θ peak at 10.62° and 23.42° with amorphic forms. Imperfect graphite oxidation during synthesis or the incoherence of the generated structures could be the cause of the difractional peak's enlargement and shift, leading to amorphous forms. Graphite raw materials originating from agricultural waste and poor graphite oxidation could be responsible for this [17]. In this study, the broad peak at 12.78° confirms the oxidation of graphite into GO due to the expansion of interlayer spacing, while the peak at 24.20° indicates residual graphitic domains. The absence of sharp peaks and the observed broadening confirm the amorphous nature of GO, characterized by disordered layers and defects that distinguish it from crystalline graphite.

3.2. Experimental Design and Optimization of DSPE using BBD

The BBD experiment lead to the execution of 29 experiments to optimize CIP adsorption. RSM model was used to look into how the adsorption of the CIP antibiotic affected four response variables: the amount of adsorbent, the pH level, the contact time, and the concentration of CIP. The goal was to examine CIP's optimization process under various scenarios. Table 2 displays the experiment's results, as well as a statistical examination of the response using quadratic statistical models from DX-13 software. The mathematical equation for the second model, shown in Equation 2, is derived from the experimental design and statistical analysis of the response using a quadratic model. A positive mark on a variable in the equation indicates that the variable has an impact on %CIP adsorption, whereas a negative mark on the variable indicates that the variant has little impact on %CIP adsorption.

$$\%\text{Adsorption} = 95.72 - 0.0123A - 2.72B - 23.22C - 2.23D + 0.0478AB + 0.5224AC - 0.1960AD - 16.16BC - 1.17BD - 10.87CD - 7.39A^2 + 2.88B^2 - 24.49C^2 + 3.10D^2 \quad (2)$$

The results obtained from the diagnostic tests shown in Fig. 4. Diagnostic tests are used to explain residual behavior following model regression. A normal distribution graph examines data against the theoretical normal diversion, with the dots forming an estimate of a straight line and deviation from the line indicating an atypical distribution. The normal distribution graph (Fig. 4(a)) shows favorable outcomes for the experiments conducted on % adsorption because the generated values align closely with the linear line of Fig. 4(b) showing a graph comparing the predicted adsorption outcome to the actual one. Generally, the experimental point is close to a straight line, showing normal distribution consistency. It also shows that the model provides an accurate prediction of experimental data. Fig. 4(c) shows a residual vs. running graph. It reveals a random distribution of data points without any discernible pattern. These diagnostics collectively support the notion that the model performs well [33]. The diagnostic test

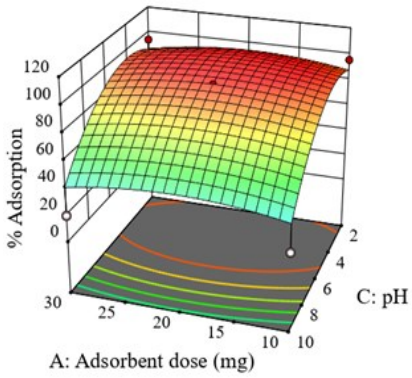

(a)

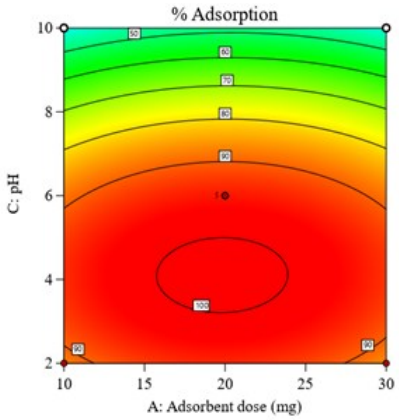

(b)

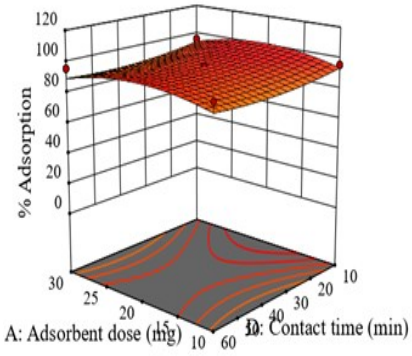

(c)

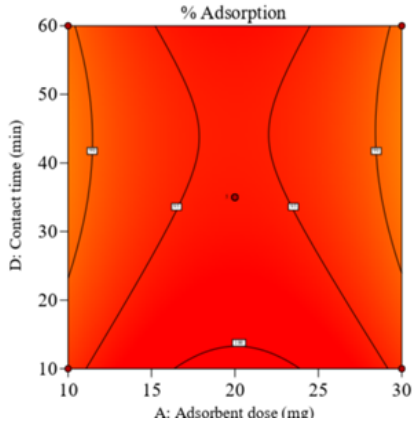

(d)

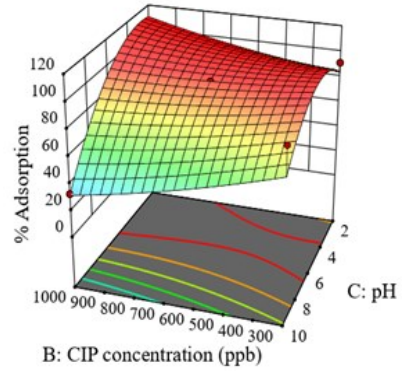

(e)

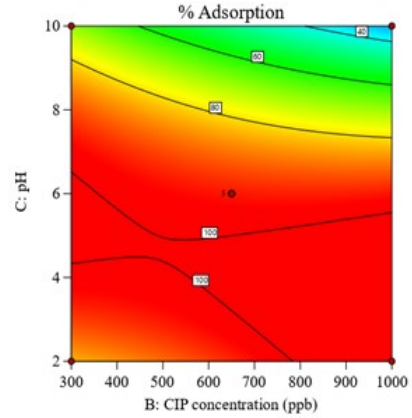

(f)

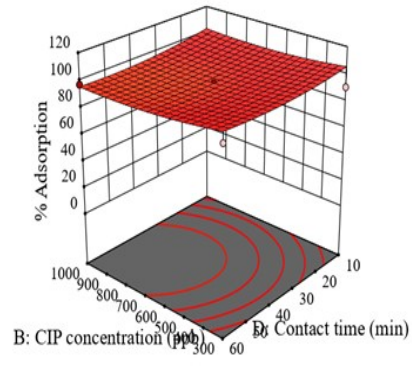

(g)

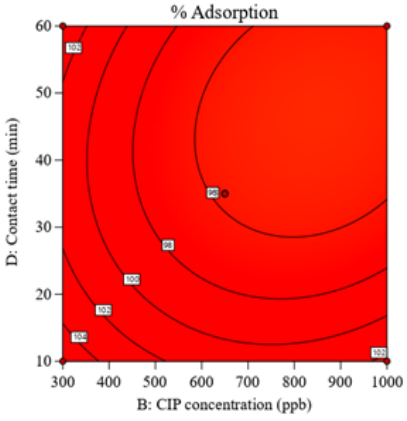

(h)

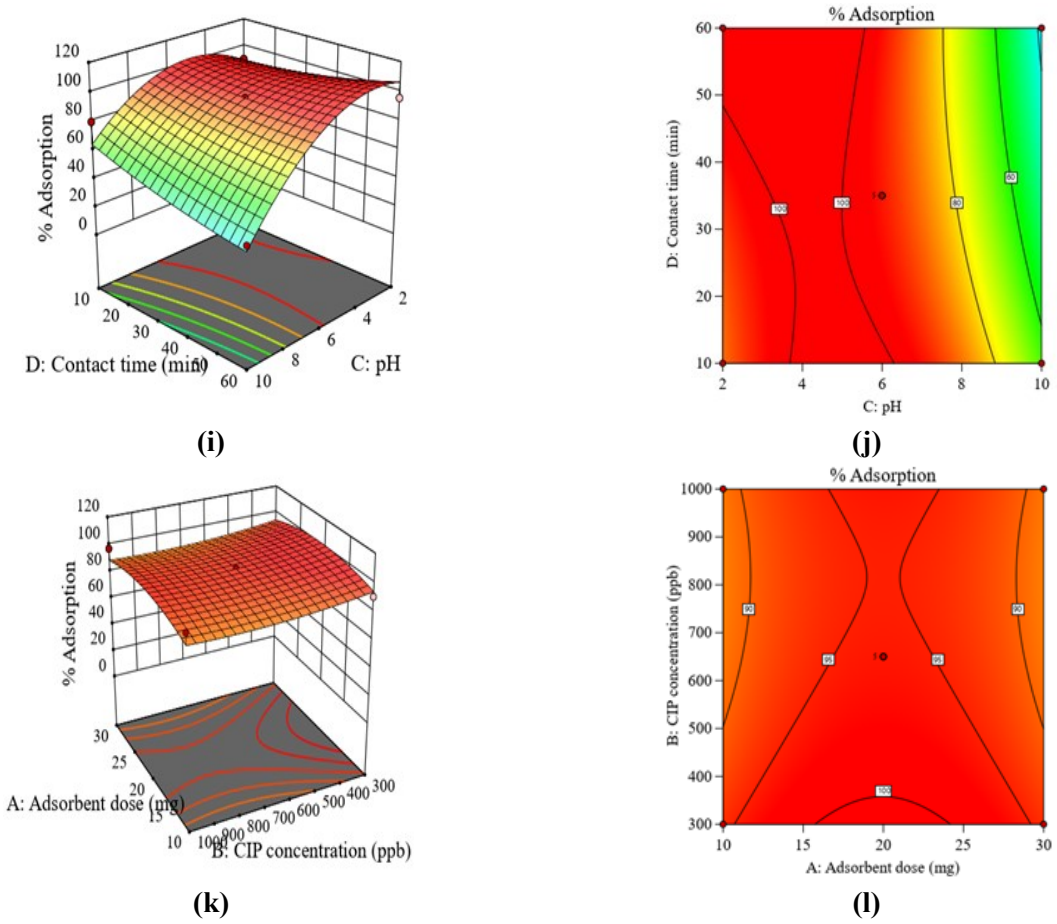

Figure 5. Response surface (3D) and contour (2D) plot: interaction between adsorbent dose and pH (a and b), interaction between adsorbent dose and contact time (c and d), interaction between CIP concentration and pH (e and f), interaction between CIP concentration dan contact time (g and h), interaction between pH and contact time (i and j), interaction between adsorbent dose and CIP concentration (k and l).

results also support the ANOVA test results obtained in Table 3. The ANOVA results show that the model is statistically significant, with 12870.91 sum square models and a P value of 0.0029 ($P < 0.05$). The P value is a standard metric used to determine the urgency of each coefficient. A P-value less than 0.05 indicates a significant and favorable model condition. Table 3 shows that the pH variable (C), the interaction of CIP concentration and pH (BC), and the pH square value (C2) shows statistical significance (P value < 0.05), indicating pH is important factor.

In comparison with previously reported dSPE methods, the performance of cassava peel–derived GO in this study is highly competitive. Nejad et al. [6] reported recoveries between 85–95% for antibiotic extraction using GO-based dSPE, while Chen et al. [23] achieved more than 90% removal efficiency for CIP using GO under optimized conditions. Similarly, Salihi et al. [12] and Rinawati et al. [10] demonstrated CIP adsorption efficiencies exceeding 90% with GO derived from synthetic and agricultural precursors, respectively. In our study, the optimized cassava peel–based GO can be reached over 95% CIP removal, which is superior to or at least comparable with these reported values, while offering the added advantage of employing a low-cost and sustainable agricultural waste source.

An adequate model condition should have an insignificant lack of fit value. However, this model produces a lack of fit value with a P value of less than 0.0001, indicating significant results. A significant lack of fit may occur if the design point variation against the projected value is substantially greater than the repeat variation toward the average value. In this study, a significant lack of fit could be attributed to the model's data variation size. The R^2 values indicate the model's ability to explain data

diversity. The R^2 value of the model is 0.8275 (Table 4). The excellent model compatibility requirement, defined as $R^2 > 0.8$ and R^2 close to 1, implies a high degree of consistency between the experimental and suggested model data. This indicates that the model has satisfactorily met the standards of an adequate model (82.75%), with only 17.25% of all variables not explained by the model. The predicted and adjusted R^2 values must deviate by less than 0.2. When the discrepancy between the predicted and adjusted R^2 values is higher than 0.2, it indicates that there may be a problem with the model or the experimental data [34]. According to the data, the difference between predicted R^2 values and R^2-adjusted values is 0.6486. The sufficient precision number is a measure of the signal's responsiveness to noise ratio. A value greater than 4 shows a strong correlation between the experimental results and the predictions made by the model. In this experiment, the accuracy value was 7.9102, which is greater than 4. This indicates that the model matches well with the experimental results and predictions. In statistical analysis, the coefficient of variation (CV) is a statistical measure that indicates the model's quality. A CV score below 10% indicates the model's level of consistency and reliability [35]. Maged et al. consider CV values exceeding 10% as acceptable, while values exceeding 30% are considered unacceptable. The model achieves a CV value of 16.29%, which is greater than 10%. This indicates that the model has an acceptable level of repeatability and reliability [28].

3.3. Interaction Effects Within Process Variables and Their Effect on CIP Removal

The three-dimensional surface plot shows the four factors' primary influence. As shown in Fig. 5 the study looked at how absorbent amount, pH, contact time, and CIP concentration affected the productivity of residual CIP adsorption. The graph shows the relationship between the amount of adsorbent (GO) and the pH level (Fig. 5 a and b). The best results were obtained when 15–23 mg of GO was in a soluble form at pH 2–6. The graph highlights these conditions in red. The best conditions for CIP adsorption are a pH range of 4–7, a concentration of 300–700 ppb, and a CIP adsorption rate of 97% (Fig. 5 e and f). The optimal conditions are a pH range of 2 to 5, a concentration higher than 780 parts per billion, and a CIP adsorption rate of over 100%. Fig. 5 i and j shows the most effective CIP adsorption settings at pH 3-5 for contact durations ranging from 10 to 60 min. The optimal conditions occurred when the pH was below 6. Otherwise, at a pH over 7, the productivity of CIP adsorption decreases by more than 90% compared to the mass of GO, contact duration, and CIP concentration.

CIP exhibits different ionic states depending on the solution pH. At pH values below 5.90, it carries a positive charge, while it predominantly exists in a neutral or zwitterionic state in the pH range of 5.90 to 8.89. When the pH exceeds 8.89, CIP shifts to a

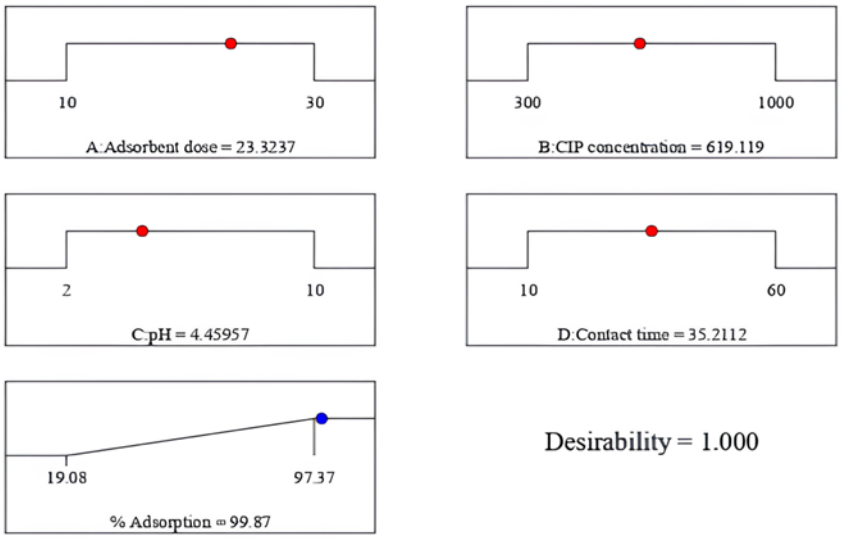

Figure 6. Ramp solution for desirability approach.

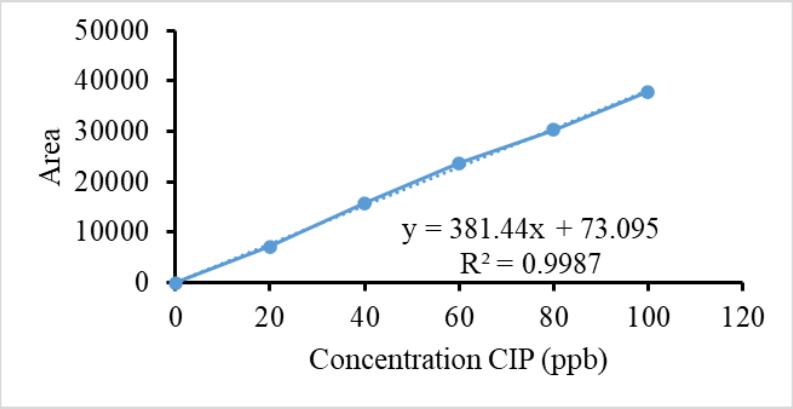

Figure 7. Curve standar calibration CIP.

negatively charged form. These protonation–deprotonation behaviors strongly influence its adsorption onto GO. The highest adsorption efficiency of CIP is generally observed under acidic to neutral pH conditions. In an acidic environment, the amine group of CIP becomes protonated (-NH_3^+), which reduces its ability to interact with the carboxyl functional groups of GO [36]. Nevertheless, at pH 5, around 80% of the carboxyl groups on GO are deprotonated (COO−), making the GO surface negatively charged. The presence of oppositely charged species under these conditions facilitates strong electrostatic attraction between GO and CIP, leading to enhanced adsorption. As the solution pH increases beyond 7, GO undergoes further deprotonation of its carboxyl groups, resulting in a more negatively charged surface. At the same time, CIP transitions into its negatively charged state, thereby creating electrostatic repulsion between the two species. This repulsive interaction significantly weakens the binding affinity of CIP toward GO, ultimately lowering the adsorption capacity of the adsorbent [23]. Therefore, the pH of the solution plays a decisive role in determining the adsorption mechanism, with acidic to near-neutral conditions being optimal for maximizing CIP removal.

The study shows that all contact times with GO masses between 17 and 22 mg achieve the optimal conditions for CIP adsorption productivity, with a rate exceeding 95%. After a duration of 26 min, the rate at which adsorption occurs begins to drop as a result of a gradual reduction in the quantity of active sites available. Eventually, the adsorbent reaches a state of saturation, resulting in a decline in the efficiency of CIP adsorption. Similarly, the relationship between the mass of GO and the concentration of CIP centers the impact Fig. 5 k and l. The most favorable conditions were obtained when the GO mass ranged from 15 to 24 mg and the CIP concentration ranged from 300 to 360 ppb. An object with a mass of less than 15 mg could not achieve CIP's ideal adsorption. This may be due to a lack of sufficient active sites at the concentration tested by CIP. When the GO mass exceeds 24 mg, it results in a decrease in CIP adsorption productivity across all evaluated CIP concentrations. This is due to the occurrence of overlapping circumstances during the adsorption process, which are attributed to the adsorbent density. These circumstances reduce the number of active sides and surface area. However, in general, a GO mass of 10–30 mg is capable of adsorbing CIP at a concentration of 300–1000 ppb, which results in a CIP adsorption productivity of over 87% [37]. Fig. 5 g and h show that the interaction effect of contact time and CIP concentration led to the best results at all contact times (10–60 min) and CIP concentrations that were tested, with CIP productivity results above 90%. All evaluated contact times at pH 3–5 resulted in an optimal condition for CIP adsorption productivity, with results surpassing 90%. Accordingly, the contact time variable has an insignificant effect on %CIP for fluctuations in CIP concentration from acidic to neutral pH.

3.4. Optimization of the Responses

An optimization research was carried out to determine the ideal combination of CIP adsorption parameters that resulted in the maximum percentage of CIP adsorption. The reaction is optimized by utilizing a desirability-based approach. Desirability

analysis calculates the total desirability by taking the geometric average of each individual desire. The desirability values span from 0 to 1. A desirability grade close to 1 reflects the high level of accuracy in the optimization process. The optimization process yields a desirability value of 1, represented visually as a ramp [34]. The diagram shown in Fig. 6. The optimization results indicate that the adsorption percentage reached its highest value at 99.87%. The optimal conditions for CIP adsorption are a pH of 4.4, a mass of 23.3237 mg of GO, a concentration of 619.119 ppb of CIP, and a contact period of 35.2112 min.

Adsorption occurs when GO and CIP engage via π-π interaction and hydrogen bonding. Also, there are two C=O groups in CIP: a fluorine group with a negative partial charge can form a hydrogen bond with a positively charged OH group on GO; and a positively charged OH group on CIP can form a hydrogen link with a negatively charged partial C=O group on GO adsorbent [38].

The calibration curve of CIP exhibited excellent linearity R^2 0.9987. The LOD and LOQ values were determined as 4.05 and 13.50 ppb, respectively, indicating the high sensitivity of the method for detecting trace levels of CIP (Fig. 7). The adsorption efficiency of the method reached up to 99.87%, which is in agreement with the optimized adsorption conditions. Furthermore, the method showed good precision, with %RSD values ranging from 3–5%, and a recovery of 98.90%, confirming its reliability and robustness for quantitative analysis.

4. CONCLUSIONS

This study demonstrates cassava peel, an abundant agricultural waste, as a sustainable and eco-friendly carbon source for the synthesis of GO. The application of RSM allowed for the simultaneous optimization of multiple parameters, resulting in a cassava peel-derived GO with enhanced adsorption properties. Characterization by FTIR, XRD, and SEM confirmed the presence of oxygen-containing functional groups, an amorphous structure, and a characteristic sheet-like morphology, indicating the successful formation of GO. Under optimized conditions (pH 4.4, 35.21 min contact time, 619.12 ppb CIP concentration, and 23.32 mg adsorbent), the material exhibited outstanding adsorption efficiency of 99.87%, alongside high analytical reliability (LOD 4.05 ppb, LOQ 13.50 ppb, %RSD 3–5%, recovery 98.90%). These findings demonstrate that cassava peel-derived GO is a highly effective, low-cost, and environmentally friendly adsorbent suitable for solid-phase DSPE applications, contributing to sustainable environmental monitoring strategies.

AUTHOR INFORMATION

Corresponding Author

Rinawati Rinawati — Departement of Chemistry, Universitas Lampung, Bandar Lampung-35145 (Indonesia);
orcid.org/0000-0002-4245-1729
Email: rinawati@fmipa.unila.ac.id

Authors

Elsa Fitrianingsih — Departement of Chemistry, Universitas Lampung, Bandar Lampung-35145 (Indonesia);
orcid.org/0000-0002-5375-352X

Dian Rifani Muthia — Departement of Chemistry, Universitas Lampung, Bandar Lampung-35145 (Indonesia);
orcid.org/0009-0003-0380-9702

Siti Salwa Khotijah — Departement of Chemistry, Universitas Lampung, Bandar Lampung-35145 (Indonesia);
orcid.org/0009-0005-2348-7231

Agung Abadi Kiswandono — Departement of Chemistry, Universitas Lampung, Bandar Lampung-35145 (Indonesia);
orcid.org/0000-0002-8145-1959

Widiarti Widiarti — Department of Mathematics, Universitas Lampung, Bandar Lampung-35145 (Indonesia);
orcid.org/0000-0002-2579-8763

Achmad Gus Fahmi — Cosmetic Engeneering Study Program, Sumatra Institute of Technology, Lampung Selatan-35635 (Indonesia);
orcid.org/0000-0002-6574-8963

Tarmizi Taher — Enviromental Engineering Study Program, Sumatra Institute of Technology, Lampung Selatan-35635 (Indonesia);
orcid.org/0000-0002-3888-7730

Author Contributions

Conceptualization, R. R.; Methodology, R. R. and E. F.; Software, E. F. and W. W.; Validation, R. R., E. F., and S. S. K.; Formal Analysis, W. W.; Investigation, T. T. and A. G. F.; Resources, R. R.; Data Curation, D. R. M.; Writing – Original Draft Preparation, R. R. and D. R. M.; Writing – Review & Editing, D. R. M. and E. F.; Visualization, A. A. K.; Supervision, Project Administration, Funding Acquisition, R. R.

Conflicts of Interest

The authors declare no conflict of interest.

ACKNOWLEDGEMENT

The author gratefully acknowledges the support of the Research Innovation and Collaboration Program (HETI) by Universitas Lampung, International Scheme program under contract numbers 9948/UN26/HK.01.03/2022.

DECLARATION OF GENERATIVE AI

Authors did not use generative AI or AI assisted technologies in the writing process.

REFERENCES

[1] A. Kutuzova, T. Dontsova, and W. Kwapinski. (2021). "Application of TiO_2-Based Photocatalysts to Antibiotics Degradation: Cases of Sulfamethoxazole, Trimethoprim and Ciprofloxacin". *Catalysts.* **11** (6): 728. 10.3390/catal11060728.

[2] C. H. Johansson, L. Janmar, and T. Backhaus. (2014). "Toxicity of Ciprofloxacin and Sulfamethoxazole to Marine Periphytic Algae and Bacteria". *Aquatic Toxicology.* **156** : 248-258. 10.1016/j.aquatox.2014.08.015.

[3] P. Kovalakova, L. Cizmas, T. J. McDonald, B. Marsalek, M. Feng, and V. K. Sharma. (2020). "Occurrence and Toxicity of Antibiotics in the Aquatic Environment: A Review". *Chemosphere.* **251**. 10.1016/j.chemosphere.2020.126351.

[4] M. Azriouil, S. Aghris, M. Matrouf, A. Benhammou, and O. Boughzala. (2022). "Efficacy of Clay Materials for Ciprofloxacin Antibiotic Analysis in Urine and Pharmaceutical Products". *Materials Chemistry and Physics.* **279**. 10.1016/j.matchemphys.2022.125787.

[5] P. K. Singh, U. Kumar, I. Kumar, A. Dwivedi, P. Singh, S. Mishra, C. S. Seth, and R. K. Sharma. (2024). "Critical review on toxic contaminants in surface water ecosystem: sources, monitoring, and its impact on human health". *Environmental Science and Pollution Research.* **31** (45): 56428-56462. 10.1007/s11356-024-34932-0.

[6] L. M. Nejad, Y. Pashaei, B. Daraei, M. Forouzesh, and M. Shekarchi. (2019). "Graphene Oxide-Based Dispersive-Solid Phase Extraction for Preconcentration and Determination of Ampicillin Sodium and Clindamycin Hydrochloride Antibiotics in Environmental Water Samples Followed by HPLC–UV Detection". *Iranian Journal of Pharmaceutical Research.* **18** (2): 642-657. 10.22037/ijpr.2019.1100676.

[7] Q. Yang, Y. Gao, J. Ke, P. L. Show, Y. Ge, Y. Liu, R. Guo, and J. Chen. (2021). "Antibiotics: An Overview on the Environmental Occurrence, Toxicity, Degradation, and Removal Methods". *Bioengineered.* **12** (1): 7376-7416. 10.1080/21655979.2021.1974657.

[8] G. J. Maranata, N. O. Surya, and A. N. Hasanah. (2021). "Optimising Factors Affecting Solid Phase Extraction Performances of Molecular Imprinted Polymer as Recent Sample Preparation Technique". *Heliyon.* **7** (5): e05934. 10.1016/j.heliyon.2021.e05934.

[9] G. Islas, I. S. Ibarra, P. Hernandez, J. M. Miranda, and A. Cepeda. (2017). "Dispersive Solid Phase Extraction for the Analysis of Veterinary Drugs Applied to Food Samples: A Review". *International Journal of Analytical Chemistry.* **2017** : 8215271. 10.1155/2017/8215271.

[10] R. Rinawati, A. Rahmawati, D. R. Muthia, M. D. Imelda, F. H. Latief, S. Mohamad, and A. A. Kiswandono. (2024). "Removal of Ceftriaxone and Ciprofloxacin Antibiotics from Aqueous Solutions Using Graphene

Oxide Derived from Corn Cob". *Global Journal of Environmental Science and Management.* **10** (3): 573-588. 10.22035/gjesm.2024.02.10.

[11] Y. A. R. Lebron, V. R. Moreira, G. P. Drumond, G. C. F. Gomes, M. M. Silva, R. O. Bernardes, R. S. Jacob, M. M. Viana, C. K. B. Vasconcelos, and L. V. S. Santos. (2020). "Statistical Physics Modeling and Optimization of Norfloxacin Adsorption onto Graphene Oxide". *Colloids and Surfaces A: Physicochemical and Engineering Aspects.* **606**. 10.1016/j.colsurfa.2020.125534.

[12] E. Ç. Salihi, J. Wang, G. Kabacaoğlu, S. Kırkulak, and L. Šiller. (2020). "Graphene Oxide as a New Generation Adsorbent for the Removal of Antibiotics from Waters". *Separation Science and Technology.* **56** (3): 453-461. 10.1080/01496395.2020.1717533.

[13] K. Murniati, W. A. Zakaria, T. Endaryanto, and L. S. M. Indah. (2021). "Analysis of production efficiency and income to support sustainability of cassava farming in Lampung Tengah District, Lampung Province". *IOP Conference Series: Earth and Environmental Science.* **739** (1). 10.1088/1755-1315/739/1/012048.

[14] F. Sulaiman, M. Septiani, S. Aliyasih, and N. Huda. (2019). "Effectiveness of a Cassava Peel Adsorbent on the Absorption of Copper (Cu^{2+}) and Zinc (Zn^{2+}) Metal Ions". *International Journal of Advanced Science, Engineering and Information Technology.* **9** (4): 1296-1301. 10.18517/ijaseit.9.4.8990.

[15] V. Kumar, A. Al-Gheethi, S. M. Asharuddin, and N. Othman. (2021). "Potential of Cassava Peels as a Sustainable Coagulant Aid for Institutional Wastewater Treatment: Characterisation, Optimisation and Techno-Economic Analysis". *Chemical Engineering Journal.* **420**. 10.1016/j.cej.2020.127642.

[16] B. P. Upoma, S. Yasmin, M. A. A. Shaikh, T. Jahan, M. A. Haque, M. Moniruzzaman, and M. H. Kabir. (2022). "A Fast Adsorption of Azithromycin on Waste-Product-Derived Graphene Oxide Induced by H-Bonding and Electrostatic Interactions". *ACS Omega.* **7** (23): 20044-20056. 10.1021/acsomega.2c01919.

[17] V. K. Gupta, S. Agarwal, M. Asif, A. Fakhri, and N. Sadeghi. (2017). "Application of Response Surface Methodology to Optimize the Adsorption Performance of a Magnetic Graphene Oxide Nanocomposite Adsorbent for Removal of Methadone from the Environment". *Journal of Colloid and Interface Science.* **497** : 193-200. 10.1016/j.jcis.2017.03.006.

[18] G. K. Khiam, R. R. Karri, N. M. Mubarak, M. Khalid, R. Walvekar, E. C. Abdullah, and M. E. Rahman. (2022). "Modelling and Optimization for Methylene Blue Adsorption Using Graphene Oxide/Chitosan Composites via Artificial Neural Network–Particle Swarm Optimization". *Materials Today Chemistry.* **24**. 10.1016/j.mtchem.2022.100946.

[19] Z. Khoshraftar, H. Masoumi, and A. Ghaemi. (2023). "Experimental, Response Surface Methodology (RSM) and Mass Transfer Modeling of Heavy Metals Elimination Using Dolomite Powder as an Economical Adsorbent". *Case Studies in Chemical and Environmental Engineering.* **7** : 100329. 10.1016/j.cscee.2023.100329.

[20] Z. Xu, Y. Zhou, Z. Sun, D. Zhang, Y. Huang, S. Gu, and W. Chen. (2020). "Understanding Reactions and Pore-Forming Mechanisms Between Waste Cotton Woven and $FeCl_3$ During the Synthesis of Magnetic Activated Carbon". *Chemosphere.* **241** : 125120. 10.1016/j.chemosphere.2019.125120.

[21] O. Akhavan, K. Bijanzad, and A. Mirsepah. (2014). "Synthesis of Graphene from Natural and Industrial Carbonaceous Wastes". *RSC Advances.* **4** (39): 20441-20448. 10.1039/c4ra01550a.

[22] F. Li, D. L. Zhao, L. Z. Bai, and D. D. Zhang. (2013). "Fabrication of Nano Hollow Graphene Oxide Spheres via Water-in-Oil Emulsion". *Applied Mechanics and Materials.* **320** : 540-543. 10.4028/www.scientific.net/AMM.320.540.

[23] H. Chen, B. Gao, and H. Li. (2015). "Removal of Sulfamethoxazole and Ciprofloxacin from Aqueous Solutions by Graphene Oxide". *Journal of Hazardous*

Materials. **282** : 201-207. 10.1016/j.jhazmat.2014.03.063.

[24] K. Elgendy, M. Zaky, T. Alaa Eldin, and S. Fadel. (2023). "Rapid HPLC Determination of Ciprofloxacin, Ofloxacin, and Marbofloxacin Alone or in a Mixture". *Results in Chemistry.* **5** : 100749. 10.1016/j.rechem.2022.100749.

[25] A. Fahmy, B. Anis, P. Szymoniak, K. Altmann, and A. Schönhals. (2022). "Graphene Oxide/Polyvinyl Alcohol-Formaldehyde Composite Loaded by Pb Ions: Structure and Electrochemical Performance". *Polymers (Basel).* **14** (11): 2303. 10.3390/polym14112303.

[26] C. S. Shivananda, S. Madhu, G. Poojitha, A. R. Sudarshan, S. Jeethendra, and K. Nagi Reddy. (2023). "Structural, Chemical and Morphological Properties of Graphite Powder, Graphene Oxide and Reduced Graphene Oxide". *Materials Today: Proceedings.* **89** : 49-53. 10.1016/j.matpr.2023.04.608.

[27] W. Kowalczuk. (2020). "FTIR Characterization of the Development of Antimicrobial Catheter Coatings Loaded with Fluoroquinolones". *Coatings.* **10** (9): 818. 10.3390/coatings10090818.

[28] M. Ali, S. Kharbish, I. S. Ismael, and A. Bhatnagar. (2020). "Characterization of Activated Bentonite Clay Mineral and the Mechanisms Underlying Its Sorption for Ciprofloxacin from Aqueous Solution". *Environmental Science and Pollution Research.* **27** : 32980-32997. 10.1007/s11356-020-09267-1.

[29] A. B. D. Nandiyanto, R. Ragadhita, and M. Fiandini. (2023). "Interpretation of Fourier Transform Infrared Spectra (FTIR): A Practical Approach in the Polymer/Plastic Thermal Decomposition". *Indonesian Journal of Science and Technology.* **8** (1): 113-126. 10.17509/ijost.v8i1.53297.

[30] E. H. Sujiono, Z. Zurnansyah, D. Zabrian, M. Y. Dahlan, B. D. Amin, S. Samnur, and J. Agus. (2020). "Graphene Oxide Based Coconut Shell Waste: Synthesis by Modified Hummers Method and Characterization". *Heliyon.* **6** (9): e04568. 10.1016/j.heliyon.2020.e04568.

[31] G. Surekha, K. V. Krishnaiah, N. Ravi, and R. P. Suvarna. (2020). "FTIR, Raman and XRD Analysis of Graphene Oxide Films Prepared by Modified Hummers Method". *Journal of Physics: Conference Series.* **1495** (1): 012012. 10.1088/1742-6596/1495/1/012012.

[32] K. Z. Donato, H. L. Tan, V. S. Marangoni, M. V. S. Martins, P. R. Ng, M. C. F. Costa, P. Jain, S. J. Lee, G. K. W. Koon, R. K. Donato, and A. H. Castro Neto. (2023). "Graphene Oxide Classification and Standardization". *Scientific Reports.* **13** : 33350. 10.1038/s41598-023-33350-5.

[33] N. Asikin-Mijan, H. V. Lee, Y. H. Taufiq-Yap, G. Abdulkrem-Alsultan, M. S. Mastuli, and H. C. Ong. (2017). "Optimization Study of SiO_2–Al_2O_3 Supported Bifunctional Acid-Base NiO–CaO for Renewable Fuel Production Using Response Surface Methodology". *Energy Conversion and Management.* **141** : 325-338. 10.1016/j.enconman.2016.09.041.

[34] S. K. Behera, H. Meena, S. Chakraborty, and B. C. Meikap. (2018). "Application of Response Surface Methodology (RSM) for Optimization of Leaching Parameters for Ash Reduction from Low-Grade Coal". *International Journal of Mining Science and Technology.* **28** (4): 621-629. 10.1016/j.ijmst.2018.04.014.

[35] A. A. M. Redhwan, W. H. Azmi, M. Z. Sharif, N. N. M. Zawawi, and S. Zainal Ariffin. (2020). "Utilization of Response Surface Method (RSM) in Optimizing Automotive Air Conditioning (AAC) Performance Exerting Al_2O_3/PAG Nanolubricant". *Journal of Physics: Conference Series.* **1532** (1): 012003. 10.1088/1742-6596/1532/1/012003.

[36] R. Rostamian and H. Behnejad. (2018). "A Comprehensive Adsorption Study and Modeling of Antibiotics as a Pharmaceutical Waste by Graphene Oxide Nanosheets". *Ecotoxicology and Environmental Safety.* **147** : 117-123. 10.1016/j.ecoenv.2017.08.019.

[37] L. Jara-Cobos, M. E. Peñafiel, C. Montero, M. Menendez, and V. Pinos-Vélez. (2023). "Ciprofloxacin Removal Using Pillared Clays". *Water (Switzerland).* **15** (11): 2056. 10.3390/w15112056.

[38] F. Gamoń, M. Tomaszewski, G. Cema, and A. Ziembińska-Buczyńska. (2022). "Adsorption of Oxytetracycline and Ciprofloxacin on Carbon-Based Nanomaterials as Affected by pH". *Archives of Environmental Protection.* **48** (4): 34-41. 10.24425/aep.2022.140764.